Journal of Solar Energy Research (JSER)

Journal homepage: www.jser.ut.ac.ir

Thermodynamic analysis of a novel solar based energy system in Tabriz

V. Beygzadeh[a*], Sh. Khalil Arya[b], I. Mirzaee[b], Gh. Miri[c], V. Zare[a]

[a] *Department of Mechanical Engineering, Faculty of Engineering, Urmia University of Technology, Iran, *Email:vbeygzadeh@gmail.com*
[b] *Department of Mechanical Engineering, faculty of engineering, Urmia University, Urmia, Iran,*
[c] *Department of Business Management, National Iranian Oil Refining & Distribution Company, Tehran, Iran,*

ARTICLE INFO

Received: 30 May 2018
Received in revised form: 10 Jul 2018
Accepted: 19 Jul 2018
Available online: 7 Aug 2018

Keywords:
Energy efficiency; exergy efficiency; solar; RORC; CHP;

A B S T R A C T

A comprehensive energy and exergy analysis is reported of a novel solar thermal CHP system for three Operation modes. Energy and exergy analyses are used to characterize the exergy destruction rate in any ingredient and estimate solar thermal CHP cycle performance. The system comprising a solar loop heat pipe evaporator, an auxiliary pump, two ORC evaporators, two storage tanks, a storage pump, a storage heat exchanger, an ORC turbine, an electrical generator, a process heat exchanger, a regenerator, a domestic water preheater (ORC cycle condenser) and an ORC pump. A computer simulation program using EES software is developed to model the solar thermal CHP system. The solar thermal CHP system simultaneously provides heating and electricity during the summer. The analysis involves the specification of effects of varying ORC evaporator pinch point, varying ambient temperature and varying ORC turbine inlet pressure on the energetic and exergetic performance of the solar thermal CHP system for three operation modes. The performance parameters calculated are exergy destruction, energetic and exergetic efficiencies. The results showed that, for the solar and solar and storages operation modes, the main source of the exergy destruction is the solar loop heat pipe evaporator and the storage mode has maximum exergy efficiency and minimum exergy destruction rate.

1. Introduction

In today's climate of growing energy needs and increasing environmental concern, alternatives to the use of nonrenewable and polluting fossil fuels have to be investigated. One such alternative is solar energy.

Solar energy is the energy obtained by capturing heat and light from the Sun. Energy from the Sun is referred to as solar energy. Technology has provided a number of ways to utilize this abundant resource. It is considered a green technology because it does not emit greenhouse gases. Solar energy is abundantly available and has been utilized since long both as electricity and as a source of heat. Combined heat and power (CHP) plants recover otherwise wasted thermal energy for heating. This is also called combined heat and power district heating.

CHP is one of the most cost efficient methods of reducing carbon emissions from heating systems in cold climates and is recognized to be the most energy efficient method of transforming energy from fossil fuels or biomass into electric power. CHP plants are commonly found in district heating systems of cities, central heating systems from buildings, hospitals, prisons and are commonly used in the industry in thermal production processes for process water, cooling, steam production or CO_2 fertilization.

Solar CHP technology, which captures and converts sunlight into both electricity and heat, reduces greenhouse gas emissions far faster than conventional solar energy systems, making it the clear choice for users committed to environmental sustainability.

A loop heat pipe is a simple device with no moving parts that can transfer large quantities of

heat over fairly large distances essentially at a constant temperature. A heat pipe is basically a sealed slender tube containing a wick structure lined on the inner surface and a small amount of fluid at the saturated state [1].

Loop heat pipes are analogous to heat pipes but have the benefit of being capable to provide trustworthy function over lengthy distance and the capability to work versus gravity fRORCe. They can carry a large heat load over a long distance. Several layouts of loop heat pipes ranging from, large size loop heat pipes to micro loop heat pipes have been developed and successfully utilized in a broad area of utilizations both ground based and space utilizations.

Iran's unique geographical position means 90% of the country has enough sun to generate solar power 300 days a year. Iran has 520 watts per hour per square meter of solar radiation every day [2].

Sunil Kumar Sansaniwal et al. [3] carried out Energy and exergy analyses of various typical solar energy applications. They showed that the energy analysis is very crucial in the study of process effectiveness while the exergetic analysis is another important tool to investigate the realistic behavior of process involving various energy losses and internal irreversibility.

Yanchao Lu and Jiangjiang Wang. [4] carried out Thermodynamics Performance Analysis of Solar-assisted Combined Cooling, Heating and Power System with Thermal Storage. They showed that when this system operates following thermal load, the system energy efficiency and COP decrease with the increase of solar energy, while exergy efficiency appears a slight fluctuation.

Anish Modi et al. [5] reviewed solar energy based heat and power generation systems. Ming Liu et al. [6] reviewed concentrating solar power plants and new developments in high temperature thermal energy storage technologies. Yunus Emre Yuksel et al. [7] performed Thermodynamic performance assessment of a novel environmentally benign solar energy based integrated system. Haichao Wanget al. [8] carried out Modelling and optimization of CHP based district heating system with renewable energy production and energy storage Man Wang, Jiangfeng Wang et al. [9] carried out Multi-objective optimization of a combined cooling, heating and power system driven by solar energy. Wei He et al. [10] carried out Theoretical investigation of the thermal performance of a novel solar loop heat pipe façade based heat pump water heating system. Xingxing Zhang et al. [11] performed Characterization of a solar photovoltaic/loop heat pipe heat pump water heating system. Xudong Zhao et al. [12] carried out Theoretical investigation of the performance of a novel loop heat pipe solar water heating system for use in Beijing, China.

In this paper, a novel solar powered CHP system equipped with a solar loop heat pipe evaporator, an auxiliary pump, two RORC evaporators, two storage tanks, a storage pump, a storage heat exchanger, an RORC turbine, an electrical generator, a process heat exchanger, a regenerator, a domestic water preheater (RORC cycle condenser) and an RORC pump is thermodynamically modelled and assessed with energy and exergy analyses for three operation modes. The primary objective are to improve understanding of this solar CHP system and proposal a new low cost, renewable and sustainable solar thermal system for cleaner production of useful energy with long time life cycle. The following specific tasks are performed:

- Model and simulate (using EES software) the solar thermal CHP system.
- Validate each part of the model and simulation.
- Perform energy and exergy analyses of the solar thermal CHP system to determine the exergy destruction rate of each ingredient and energy and exergy efficiencies of the entire system.
- Execute a comprehensive parametric study to determine the effect of major design parameters on system performance.

The system description and assumptions are presented next. Then, system modeling, results and discussion, and conclusions are presented, respectively.

2. Materials and Methods

In this section, the specifications of the solar thermal CHP system and its ingredients for three operation modes are introduced.

2.1. System description

Fig. 1 indicates a CHP system comprising a solar loop heat pipe evaporator, an auxiliary pump, two RORC evaporators, two storage tanks, a storage heat exchanger, a storage pump, an RORC turbine, an electrical generator, a process heat exchanger, a regenerator, a domestic water preheater (RORC cycle condenser) and an RORC pump. This solar CHP system uses the solar energy under Tabriz summer conditions to evaporate a working fluid (toluene in this study, with the thermodynamic properties listed in Table 1) through the solar loop heat pipe evaporator, which drives RRORC evaporator and vaporize regenerative organic Rankine cycle working fluid (A typical organic fluid used in RRORC is n-hexane, with the thermodynamic properties listed in Table 1).

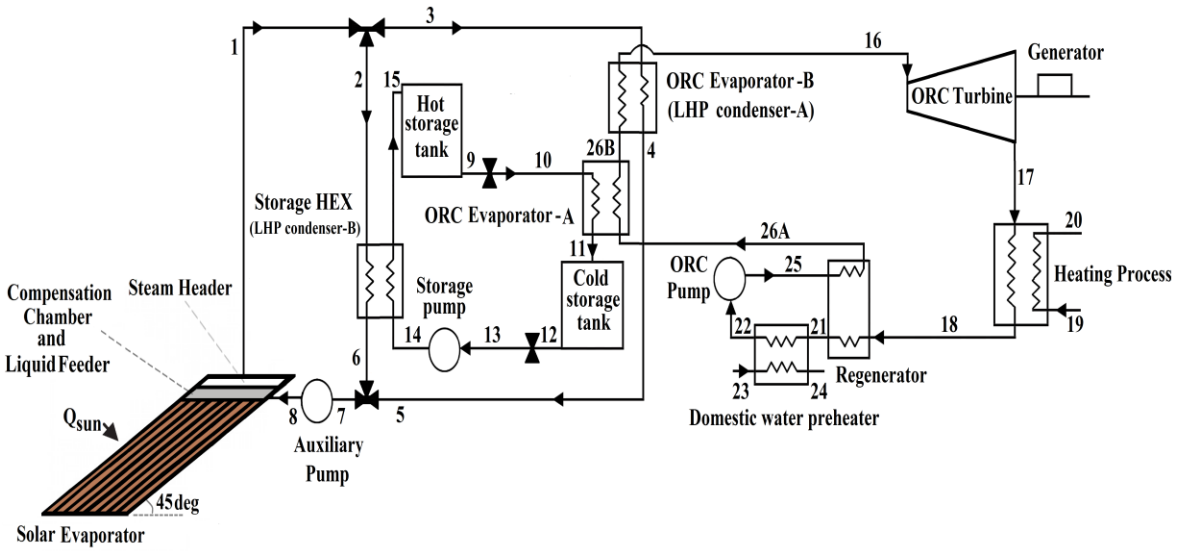

Figure 1. Schematic of the proposed system

Table 1. Properties of working fluids for the solar CHP system			
Properties of toluene (working fluid for SLHPS)		Properties of n-hexane (working fluid for RRORC)	
Parameter	Value	Parameter	Value
Chemical formula	C_7H_8	Chemical formula	C_6H_{14}
Molar mass (kg/kmol)	92.14	Molar mass (kg/kmol)	86.18
Boiling temperature (^oC)	111	Boiling temperature (^oC)	68.5 to 69.1
Density (kg/m3)	867	Density (kg/m3)	655
Freezing temperature (^oC)	−95	Freezing temperature (^oC)	−96 to −94
Critical temperature (^oC)	318.6	Critical temperature (^oC)	234.7
Critical pressure (MPa)	4.126	Critical pressure (MPa)	3.058

N-hexane superheated vapour after leaving RRORC evaporator enters to the RRORC turbine to produce electricity. After passing through the turbine, the waste heat from the RRORC is utilized to produce hot water in the heating process via the process heat exchanger. At the outlet of the process heat exchanger (point 18) since the working fluid has not reached the two phase state and its temperature at this point is higher than the condensing temperature, this higher temperature fluid used to preheat the liquid (RRORC working fluid) before entering to the RRORC evaporator. The vapor is then condensed in a domestic water preheater (RRORC condenser) for warm water production. The working fluid is then pumped to the regenerator and after absorbing heat, streams to the RRORC evaporator and the cycle is repeated continuously

The solar loop heat pipe system, is composed of solar evaporator (which is consist of 6725 wicked loop heat pipes for the solar mode and 6935 wicked loop heat pipes for the solar and storage mode), vapour and liquid lines, vapour and liquid headers, compensation chamber, as well as a plate heat exchanger (RRORC evaporator). The loop heat pipes evaporators are located on a low content of Ferro oxide glass plate in parallel lines with a small gap in among. In exploitation, the received solar energy transforms the toluene on the wicks of the loop heat pipes into vapour, which streams along the loop heat pipes to the vapour header, due to the buoyancy of vapour, auxiliary pump pressure and the gravity fRORCe created by the altitude discrepancy between the RORC evaporator and the solar evaporator (points 4 and 5 in Fig. 1). The vapour is then hauled to RRORC evaporator through the vapour line.

Through the liquid line, the toluene liquid enters the auxiliary pump. The auxiliary pump increases the pressure of SLHPS working fluid and working fluid enters the compensation chamber

placed under the vapour header. This amount of liquid is then divided to all loop heat pipes evaporators through a liquid feeder fixed at the over sector of the solar loop heat pipe evaporator, as shown in Fig. 1. The liquid feeder would let the liquid to be descended into the loop heat pipes wicks equally. The schematic of LHP is shown in Fig. 2.

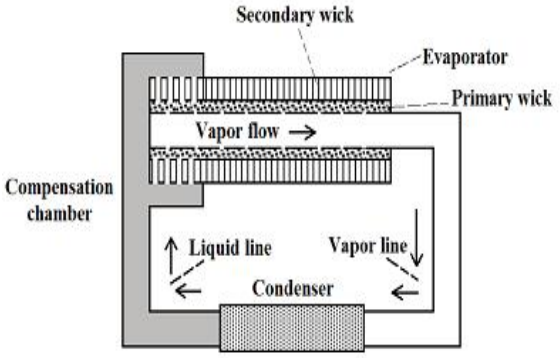

Figure 2. The schematic of LHP

The loop heat pipe system as well as uses a three path structure to supply rapid liquid distribution in the loop heat pipes evaporator wicks, as shown in Fig. 3.

Because the solar radiation varies in a 24 hours of day, the solar thermal CHP system investigated in this study is supposed to work in three modes: solar, solar and storage, and storage modes. After the sun-up, and before the evening, all the solar energy prepared by the LHPs is applied to drive the CHP system. This mode is named the solar mode (7:00 am to 9:00 am and 17:00 pm to 19:00 pm). At the other time of the day (high solar radiation time), part of the solar energy prepared by the LHPs is applied to drive the CHP system. The remaining part of the solar energy is stored in the thermal storage tank. This mode is named the solar and storage mode (9:00 am to 17:00 pm) 60% of the solar energy prepared during the solar and storage mode is stored in the thermal storage tank. This percentage is selected based on the ratio of solar and storage mode time to storage mode time. At night time, the CHP system drives using the energy stored in the thermal storage. This mode is called the storage mode (19:00 pm to 7:00 am). The thermal storage subsystem stores the surplus solar energy during the day time and, therefore, ensures running the system at night time (In this study, the two thermal storage tanks is selected). These three modes are selected based on the change in solar radiation densities. The solar radiation densities are for average annual conditions for Tabriz, Iran.

Fig.4. Shows the change of the solar radiation density during the day time for Tabriz, Iran as well as three modes of operation for CHP system.

To carry out the thermodynamic analysis and comparison of the proposed system, this presumptions are used:

- All the processes are considered to be operating at steady state.
- Heat losses from piping and other components are insignificant.
- Thermal and radiation properties of the solar loop heat pipe evaporator are considered independent of temperature.
- All of the solar loop heat pipe system components are adiabatic except loop heat pipes evaporators.
- The flow regime in the SLHPS is laminar.
- Pressure drop in vapour and liquid headers was neglected.
- Pressure drops in vapour and liquid lines are neglected.
- Pressure drop in compensation chamber was neglected.
- Exergy destruction by hot storage tank valve was neglected.
- Exergy destruction by cold storage tank valve was neglected.
- The dead state pressure is 101kPa.
- The dead state temperature is 298.15 K.
- The ambient temperature is 301.15 K.
- Pressure drops in RRORC cycle are negligible.
- The average solar radiation during the solar mode operation period of 7:00 until 9:00 and 17:00 until 19:00 was 250 W/m2 (under Tabriz summer conditions).
- The average solar radiation during the solar and storage mode operation period of 9:00 until 17:00 was 600 W/m2 (under Tabriz summer conditions).
- There is an axisymmetric stream in all the parts of the SLHPS.
- There is an axisymmetric stream in all the parts of the SLHPS.
-

2.2. Thermodynamic modeling

For thermodynamic modeling, the proposed system (Fig. 1) is divided into two Main parts: solar system and RRORC cycle. The equations

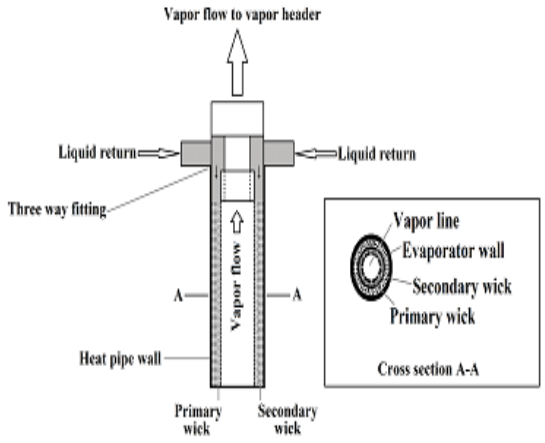

Figure 3. Schematic of three-way feeding and vapour /liquid separation structure

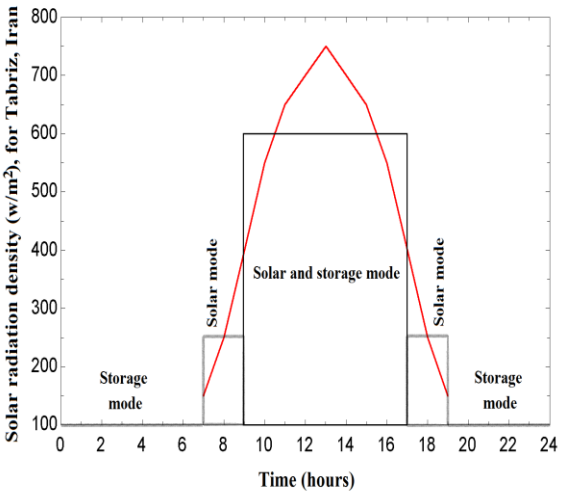

Figure 4. The change of the solar radiation density during the day time for Tabriz, Iran as well as three modes of operation for the proposed CHP system

developed are programmed using Engineering Equation Solver (EES) software. The input data used in this model are given in Table 2 and Table 3.

We specify the input and output enthalpy and exergy streams, exergy destruction rates and energy and exergy efficiencies. The energy balances and governing equations for the main sections of the proposed systems are described in the following subsections.

Table 2. Input data for the CHP system	
Turbines efficiency	85%
Pumps efficiency	85%
Working fluid	n-hexane
RRORC evaporator pinch point, ^{0}C	2
Heating process heat exchanger pinch point, ^{0}C	2
RRORC turbine inlet temperature, ^{0}C	119.7
RRORC pump inlet pressure, kPa	20
RRORC turbine inlet pressure, kPa	350
Domestic water preheater pinch point, ^{0}C	4
Process heat exchanger type	Plate heat exchanger
RRORC evaporator type	Plate heat exchanger
Domestic water preheater type	Plate heat exchanger

2.3. Mass, energy and exergy analysis

Mass, energy and exergy balances for any control volume at steady state operation with negligible potential and kinetic energy changes can be expressed, respectively, by

$$\sum_k \dot{m}_i - \sum_k \dot{m}_e = \frac{dm_{cv}}{dt} \quad (1)$$

$$\frac{dE_{cv}}{dt} = \sum \dot{Q}_{cv} - \dot{W}_{cv} + \sum_i \dot{m}_i h_i - \sum_e \dot{m}_e h_e \quad (2)$$

$$\frac{d\psi_{cv}}{dt} = \sum_i \dot{m}_i \psi_i - \sum_e \dot{m}_e \psi_e + \sum_j (1 - \frac{T_0}{T_J}) \dot{Q}_j - (\dot{W}_{cv} - P_0 \frac{dV_{cv}}{dt}) - \dot{I}_{cv} \quad (3)$$

The specific exergy is given by

$$\psi = (h - h_0) - T_0 (s - s_0) \quad (4)$$

Then the total exergy rate associated with a fluid stream becomes

$$\dot{E} = \dot{m}\psi \quad (5)$$

The relevant mass, energy and exergy balances and governing equations for the main sections of the CHP systems shown in Fig. 1 are described in the following subsections.

2.4. Solar loop heat pipe system

In the solar loop heat pipe systems with auxiliary pump, the system heat transfer capacity will be controlled by five limits (sonic, entrainment, viscous, boiling and liquid filling mass limits) the minim values of this limitations

will be the actual retention of the solar loop heat pipe system heat transfer. The value of this limits are related to the thermal properties of the working fluids, loop heat pipes structure and loop heat pipes working conditions.

Table 3. Input data for the solar loop heat pipe system	
Solar evaporator length, (m)	1.5
LHPs wicks length, (m)	1.5
LHPs evaporators length, (m)	1.5
Solar evaporator slope	45°
Overall heat loss coefficient from LHP to ambient (kW/m^2)	0.005
Overall heat loss coefficient from LHP fluid to ambient (kW/m^2)	0.0045
Liquid filling mass, (kg)	4.568
Critical radius of bubble generation for toluene, (m)	0.00000007
Solar evaporator heat removal factor	0.83
Solar evaporator to heat exchanger height difference	1
LHPs material	Black Nickel
Solar evaporator optical efficiency	0.8736
SLHPS heat exchanger height, (m)	2
Solar system operating temperature range	100-127 ^{o}C
SLHPS condensers length, (m)	2
LHPs mesh ratio (PWM/SWM)	2:1
Hot storage tank temperature drop, ^{o}C	5
RRORC evaporator operating pressure range, (kPa)	0-4500
Cold storage tank temperature drop, ^{o}C	3
LHPs type	Mesh screen
LHPs layers	Two layers
Storage heat exchanger (plate heat exchanger) pinch point, ^{o}C	2
number of LHPs for the solar mode	6725
number of LHPs for the solar and storage mode	6935
Thickness of LHPs wicks, (m)	0.0075
Thickness of LHPs secondary wicks, (m)	0.005
LHPs porosity	0.64
Internal diameter of LHPs, (m)	0.049
Thickness of LHPs primary wicks, (m)	0.0025
External diameter of LHPs evaporators, (m)	0.05
Effective diameter of wicks pores, (m)	0.1111
Number of wicks pores	9
Internal diameter of LHPs wicks vapour lines (m)	0.041
RRORC evaporator conductivity, ($W/m.K$)	16
SLHPS Vapour header material	Black Nickel
SLHPS vapour line material	Cast iron
Thermal conductivity of evaporator wall, ($W/m.K$)	91
Thermal conductivity of evaporator wick,($W/m.K$)	91
SLHPS liquid line material	Cast iron
LHPs walls thickness, (m)	0.001
SLHPS vapour line diameter, (m)	0.6
Solar evaporator vapour pressure drop, (kPa)	7
SLHPS liquid line diameter, (m)	0.5
SLHPS liquid line length (m)	4
Solar evaporator liquid pressure drop, (kPa)	4
Low content of Ferro oxide glass transmission factor, (τ)	0.91
SLHPS vapour line thickness, (m)	0.002
Black nickel absorption factor (α)	0.96
RRORC evaporator (SLHPS condenser) vapour pressure drop, (kPa)	5
RRORC evaporator (SLHPS condenser) liquid pressure drop, (kPa)	1
SLHPS average stream speed, (m/s)	50
SLHPS liquid line thickness, (m)	0.002
SLHPS vapour line Length, (m)	3
Gravity effect pressure, (kPa)	+14.936

According to Xingxing Zhang et al. [13], the heat transfer limits of the solar loop heat pipe system is shown in Table 4.

The thermodynamic analysis of the solar loop heat pipe system are presented in this subsection. To model the solar loop heat pipe system, we consider the method used by John A. Duffie et al. [14].

2.4.1. Solar mode

- Solar loop heat pipe evaporator

As shown in Fig. 1, toluene enters the solar loop heat pipe system (solar loop heat pipe evaporator) at point 8 and is heated by the solar loop heat pipe evaporator. The useful heat gained by the working fluid can be written as:

$$\dot{Q}_u = \dot{m}_1(h_1 - h_8) \quad (6)$$

Where h_1, h_8 and $\dot{m}_1$ are the toluene outlet enthalpy, inlet enthalpy and mass flow rate. The useful power produced by the solar loop heat pipe system is calculated as

$$\dot{Q}_u = A_{SOL,EVA} F_R (S - U_l (T_8 - T_{amb})) \quad (7)$$

Where T_{amb} is the ambient temperature, $A_{SOL,EVA}$ is the solar loop heat pipe evaporator effective area and can be expressed as

$$A_{SOL,EVA} = 0.75 \times N_{LHP} \pi D_o L_e \quad (8)$$

Table 4. The operating limits of the solar loop heat pipe system

Operating limits	Solar mode	Solar and storage mode
Entrainment limit $\dot{Q}_{EL}(kW)$	2568	2648
Viscous limit $\dot{Q}_{VL}(kW)$	51379	52983
Sonic limit $\dot{Q}_{SL}(kW)$	309323	318982
Boiling limit $\dot{Q}_{BL}(kW)$	1133000	1169000
Filled liquid Mass limit $\dot{Q}_{FL}(kW)$	1032	1032

and the F_R is heat removal factor which is around 0.83 for this case and U_l is the overall solar evaporator heat loss coefficient. In Eq. (7), radiation flux absorbed by the solar loop heat pipe evaporator is calculated as:

$$S = \eta_{LHP} G_b \quad (9)$$

where G_b is the solar radiation and η_{LHP} is the LHP optical efficiency and defined as:

$$\eta_{LHP} = \tau\alpha \quad (10)$$

where τ is the low content of Ferro oxide glass transmission factor and α is the black nickel absorption factor.

The energy efficiency of the solar evaporator is expressed as

$$\eta_{en,SOL,EVA} = \frac{\dot{Q}_u}{G_b A_{SOL,EVA}} \quad (11)$$

The exergy of a solar loop heat pipe evaporator is defined as

$$\dot{E}_{SUN} = G_b A_{SOL,EVA} (1 + \frac{1}{3}(\frac{T_{amb}}{T_{SUN}})^4 - \frac{4}{3}(\frac{T_{amb}}{T_{SUN}})) \quad (12)$$

where T_{SUN} is the sun temperature and equals to 4500 K.

The exergy destruction of the solar loop heat pipe evaporator is

$$\dot{I}_{SOL,EVA} = \dot{E}_8 - \dot{E}_1 + \dot{E}_{SUN} \quad (13)$$

- Auxiliary pump

The auxiliary pump work can be expressed using an energy rate balance for a control volume around the auxiliary pump as follows:

$$\dot{W}_{AUX,Pump} = \dot{m}_8 (h_8 - h_7) \quad (14)$$

The auxiliary pump exergy balance can be expressed as

$$\dot{I}_{AUX,PUMP} = \dot{E}_7 + \dot{W}_{AUX,Pump} - \dot{E}_8 \quad (15)$$

- RORC evaporator B

To determine the temperature and enthalpy for flows through the RORC evaporator, the following energy balance can be applied to the evaporator:

$$\dot{m}_3 (h_3 - h_4) = \dot{m}_{16} (h_{16} - h_{26}) \quad (16)$$

The RORC evaporator exergy balance can be expressed as

$$\dot{I}_{ORC,EVA} = \dot{E}_3 + \dot{E}_{26} - \dot{E}_{16} - \dot{E}_4 \quad (17)$$

2.4.2. Solar and storage mode

- Solar loop heat pipe evaporator

Thermodynamic modelling of the solar loop heat pipe evaporator was already explained in details in section 2.4.1. Same thermodynamic modelling is considered for the solar and storage mode.

- Auxiliary pump

Mass balance for the auxiliary pump can be written as

$$\dot{m}_8 = \dot{m}_7 = \dot{m}_5 + \dot{m}_6 \quad (18)$$

The auxiliary pump work can be expressed using an energy rate balance for a control volume around the auxiliary pump as follows:

$$\dot{W}_{AUX,Pump} = \dot{m}_8 (h_8 - h_7) \quad (19)$$

Here, h_7 is the auxiliary pump enthalpy, which is calculated as

$$h_7 = \frac{\dot{m}_6 h_6 + \dot{m}_5 h_5}{\dot{m}_7} \quad (20)$$

The auxiliary pump exergy balance can be expressed as

$$\dot{I}_{AUX,PUMP} = \dot{E}_7 + \dot{W}_{AUX,Pump} - \dot{E}_8 \quad (21)$$

- RORC evaporator B

Thermodynamic modelling of the RORC evaporator was already explained in details in section 2.4.1. Same thermodynamic modelling is considered for the solar and storage mode.

- Storage heat exchanger

Mass balance for the storage heat exchanger can be written as

$$\dot{m}_2 = \frac{3}{2}\dot{m}_3 \quad (22)$$

$$\dot{m}_2 = \dot{m}_1 - \dot{m}_3 \quad (23)$$

$$\dot{m}_{14} = \dot{m}_2 \quad (24)$$

$$\dot{m}_{15} = \dot{m}_{14} \quad (25)$$

To determine the temperature and enthalpy for flows through the storage heat exchanger, the following energy balance can be applied to the storage heat exchanger:

$$\dot{m}_2(h_2 - h_6) = \dot{m}_{14}(h_{15} - h_{14}) \quad (26)$$

The storage heat exchanger exergy balance can be expressed as

$$\dot{I}_{ST,HEX} = \dot{E}_2 + \dot{E}_{14} - \dot{E}_6 - \dot{E}_{15} \quad (27)$$

2.4.3. Storage mode

- Storage heat exchanger

Thermodynamic modelling of the storage heat exchanger was already explained in details in section 2.4.2. Same thermodynamic modelling is considered for the storage mode.

- Hot storage tank

The saturated vapour leaving the hot storage tank at point 40 enters the RORC evaporator. A mass balance for the hot storage tank can be written as

$$\dot{m}_9 T_{CH,CST} = \dot{m}_{15} T_{CH,HST} \quad (28)$$

In the hot storage tank, due to heat loss from the hot storage tank, $5\,^{o}C$ temperature drop is considered.

$$T_9 = T_{15} - 5 \quad (29)$$

The exergy destruction of the hot storage tank is

$$\dot{I}_{HST} = \dot{E}_{15} - \dot{E}_9 \quad (30)$$

- Hot storage tank valve

A mass balance for the hot storage tank valve can be written as

$$\dot{m}_{10} = \dot{m}_9 \quad (31)$$

An energy balance for the hot storage tank valve can be expressed as

$$h_{10} = h_9 \quad (32)$$

An exergy balance for the hot storage tank valve can be expressed as

$$\dot{E}_{10} = \dot{E}_9 \quad (33)$$

- Cold storage tank

The saturated liquid leaving the RORC evaporator at point 11 enters the cold storage tank. A mass balance for the cold storage tank can be written as

$$\dot{m}_{11} T_{CH,CST} = \dot{m}_{12} T_{CH,HST} \quad (34)$$

In the cold storage tank, due to heat loss from the cold storage tank, $3\,^{o}C$ temperature drop is considered.

$$T_{12} = T_{11} - 3 \quad (35)$$

The exergy destruction of the cold storage tank is

- Cold storage tank valve

A mass balance for the cold storage tank valve can be written as

$$\dot{m}_{13} = \dot{m}_{12} \quad (36)$$

An energy balance for the cold storage tank valve can be expressed as

$$h_{13} = h_{12} \quad (37)$$

An exergy balance for the cold storage tank valve can be expressed as

$$\dot{E}_{13} = \dot{E}_{12} \quad (38)$$

- Storage pump

The storage pump work can be expressed using an energy rate balance for a control volume around the storage pump as follows:

$$\dot{W}_{ST,PUMP} = \dot{m}_{14}(h_{14} - h_{13}) \quad (39)$$

The storage pump exergy balance can be expressed as

$$\dot{I}_{ST,PUMP} = \dot{E}_{13} + \dot{W}_{AUX,Pump} - \dot{E}_{14} \quad (40)$$

- RORC evaporator A

To determine the temperature and enthalpy for flows through the RORC evaporator, the following energy balance can be applied to the evaporator:

$$\dot{m}_{10}(h_{10} - h_{11}) = \dot{m}_{16}(h_{16} - h_{26}) \quad (41)$$

The RORC evaporator exergy balance can be expressed as

$$\dot{I}_{ORC,EVA} = \dot{E}_{26} + \dot{E}_{10} - \dot{E}_{11} - \dot{E}_{16} \quad (42)$$

2.4.4. Validation of the solar evaporator model

The solar evaporator model is validated against the experimental study by E. Azad [15], as shown in Fig. 5. The model demonstrates good agreement with the experimental work. The little deviation in the simulations as compared to the experimental results is due to the systems modeling conditions (for example, ambient temperature).

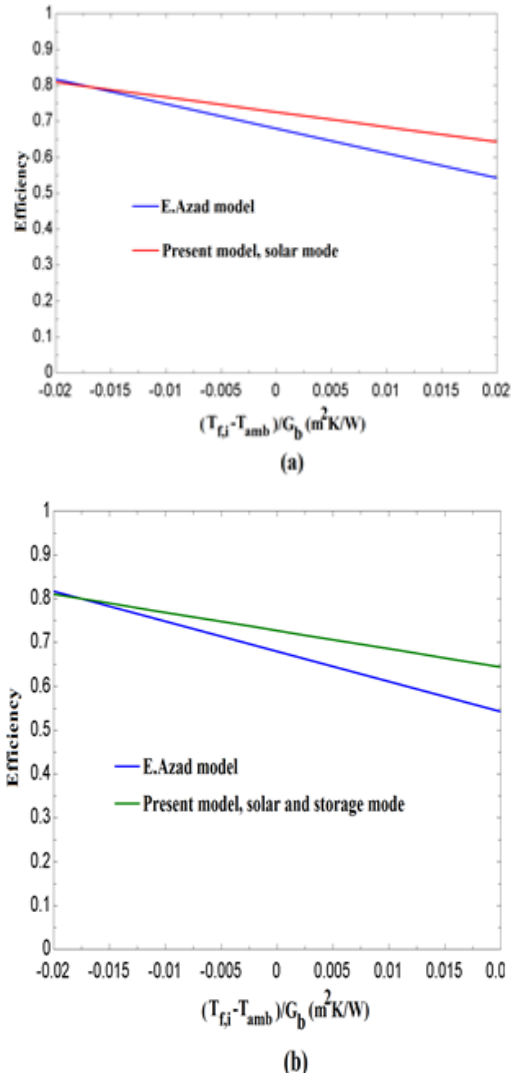

Figure 5. Validation of the solar evaporator model as compared with E. Azad [15] (a) solar mode, (b solar and storage mode

2.5. CHP cycle

The superheated n-hexane vapour leaving the RRORC evaporator enters to the CHP cycle to produce heating, cooling and electricity. Energy balances and governing equation for all ingredients of CHP cycle are provided below.

- RRORC Turbine

An energy balance for RRORC turbine can be written as

$$\dot{W}_{ORC,T} = \dot{m}_{16}(h_{16} - h_{17}) \quad (43)$$

An exergy balance for the RRORC turbine can be expressed as

$$\dot{I}_{ORC,T} = \dot{E}_{16} - \dot{E}_{17} - \dot{W}_{ORC,T} \quad (44)$$

- Process heat exchanger

The n-hexane vapour from the RRORC turbine enters the process heat exchanger to produce process hot water. The energy and exergy balance for this ingredient can be expressed, respectively, by

$$\dot{m}_{17}(h_{17} - h_{18}) = \dot{m}_{HP}(h_{20} - h_{19}) \quad (45)$$

$$\dot{I}_{HP} = \dot{E}_{17} + \dot{E}_{19} - \dot{E}_{18} - \dot{E}_{20} \quad (46)$$

- Regenerator

The n-hexane vapour from the process heat exchanger enters the regenerator to warm RORC cycle working fluid after leaving the RORC pump. The energy and exergy balances for this ingredient can be expressed, respectively, by

$$\dot{m}_{18}(h_{18} - h_{21}) = \dot{m}_{25}(h_{26} - h_{25}) \quad (47)$$

$$\dot{I}_{REG} = \dot{E}_{18} + \dot{E}_{25} - \dot{E}_{21} - \dot{E}_{26} \quad (48)$$

- Domestic water preheater

The n-hexane flow from the regenerator enters the domestic water preheater to warm domestic water. The energy and exergy balances for this ingredient can be expressed, respectively, by

$$\dot{m}_{21}(h_{21} - h_{22}) = \dot{m}_{DWPH}(h_{24} - h_{23}) \quad (49)$$

$$\dot{I}_{DWPH} = \dot{E}_{21} + \dot{E}_{23} - \dot{E}_{22} - \dot{E}_{24} \quad (50)$$

- RORC pump

The RORC pump work can be expressed using an energy rate balance for a control volume around the RORC pump as follows:

$$\dot{W}_{ORC,P} = \dot{m}_{25}(h_{25} - h_{22}) \quad (51)$$

The RORC pump exergy balance can be expressed as

$$\dot{I}_{ORC,P} = \dot{E}_{22} + \dot{W}_{ORC,P} - \dot{E}_{25} \quad (52)$$

2.5.1. Validation of the CHP cycle model

Since there was no theoretical and experimental study in field of solar loop heat pipe evaporator based CHP systems, the analysis of the CHP cycle is validated with the U.S. Department of Energy's Office of Energy Efficiency and

Renewable Energy data, as shown in Table 5. The results show a very good agreement between the current CHP system model and the U.S. Department of Energy data.

Table 5. Validation of the CHP system model		
U.S. Department of Energy data	Present study (solar mode)	Present study (solar and storage mode)
Overall CHP cycle reasonable efficiency: 65-75%	Overall CHP cycle efficiency: 71.72%	Overall CHP cycle efficiency: 72.58%

2.6. Overall analysis of the proposed system

The energy efficiency of the CHP system for the solar mode is defined as

$$\eta_{en} = \frac{\dot{Q}_{HP} + \dot{Q}_{DWPH} + \dot{W}_{Net.T}}{G_b A_{SOL,EVA}} \quad (53)$$

The exergy efficiency of the CHP system for the solar mode is defined as

$$\eta_{ex} = \frac{\dot{W}_{Net.T} + \dot{E}_{DWPH,out} - \dot{E}_{DWPH,in} + \dot{E}_{HP,out} - \dot{E}_{HP,in}}{\dot{E}_{SUN}} \quad (54)$$

Here, $\dot{E}_{SUN}$ is the total inlet exergy to the CHP system.

The energy efficiency of the CHP system for the solar and storage mode is defined as

$$\eta_{en} = \frac{\dot{Q}_{ST,HEX} + \dot{Q}_{HP} + \dot{Q}_{DWPH} + \dot{W}_{Net.T}}{G_b A_{SOL,EVA}} \quad (55)$$

The exergy efficiency of the CHP system for the solar and storage mode is defined as

$$\eta_{ex} = \frac{\dot{W}_{Net.T} + \dot{E}_{DWPH,out} - \dot{E}_{DWPH,in} + \dot{E}_{HP,out} - \dot{E}_{HP,in} + \dot{E}_{15} - \dot{E}_{14}}{\dot{E}_{SUN}} \quad (56)$$

Here, $\dot{E}_{SUN}$ is the total inlet exergy to the CHP system.

The energy efficiency of the CHP system for the storage mode is defined as

$$\eta_{en} = \frac{\dot{Q}_{HP} + \dot{Q}_{DWPH} + \dot{W}_{Net.T}}{\dot{m}_2 (h_2 - h_6)} \quad (57)$$

The exergy efficiency of the CHP system for the storage mode is defined as

$$\eta_{ex} = \frac{\dot{W}_{Net.T} + \dot{E}_{DWPH,out} - \dot{E}_{DWPH,in} + \dot{E}_{HP,out} - \dot{E}_{HP,in}}{\dot{E}_2 - \dot{E}_6} \quad (58)$$

Here, $(\dot{E}_2 - \dot{E}_6)$ is the total inlet exergy to the CHP system.

1. Results & Discussion

The solar thermal CHP system was analyzed using the above equations noting that the environment reference pressure and temperature are 101kPA and 298.15K, respectively. The energy analysis results are summarized in Table 6, Table 7 and Table 8. The energy analysis shows the energy transfer of each ingredient of the proposed system and the energy efficiency of the solar CHP system.

Table 6. The results of energy analysis of the CHP system for the solar mode	
Solar evaporator useful energy	213.1 kW
Heating process energy flow	31.64 kW
Domestic water preheater energy flow	148.3 kW
Regenerator energy flow	1.58 kW
RORC evaporator energy flow	213.1 kW
RORC turbine net power	33.18 kW
RORC pump input power	0.2414 kW
Auxiliary pump input power	0.001131 kW
CHP cycle efficiency	71.72%

Table 7. The results of energy analysis of the CHP system for the solar and storage mode	
Solar evaporator useful energy	533.7 kW
Heating process energy flow	31.64 kW
Domestic water preheater energy flow	148.3 kW
Storage heat exchanger energy flow	320.6 kW
Regenerator energy flow	1.58 kW
RORC evaporator energy flow	213.1 kW
RORC turbine net power	33.17 kW
RORC pump input power	0.2414 kW
Auxiliary pump input power	0.00894 kW
CHP cycle efficiency	72.58%

The exergy analysis results are summarized in Table 9, Table 10 and Table 11 and show that the highest exergy destruction rate happens in the solar loop heat pipe evaporator for the solar and solar and storage operation modes. The principal proof of this major exergy destruction rate is the large temperature discrepancy in the solar evaporator. As showed above, the major source of exergy destruction is the solar loop heat pipe evaporator and, thus, it needs precise design to improve its performance. The results also showed that the storage mode has maximum exergy efficiency and

minimum exergy destruction rate. Since the storage mode prime mover is the storage heat exchanger and other operation modes prime mover is the solar loop heat evaporator and the exergy destruction rate in the solar loop heat pipe evaporator is much higher than in storage heat exchanger.

Table 8. The results of energy analysis of the CHP system for the storage mode	
Storage heat exchanger useful energy	320.6 kW
Heating process energy flow	27.97 kW
Domestic water preheater energy flow	148.3 kW
Regenerator energy flow	1.58 kW
RORC evaporator energy flow	208.9 kW
RORC turbine net power	32.56 kW
RORC pump input power	0.2414 kW
Storage pump input power	0.0992 kW
CHP cycle efficiency	65.13%

Table 9. The results of exergy analysis of the CHP system for the solar mode	
Solar evaporator exergy destruction rate	224.7 kW
RORC evaporator exergy destruction rate	5.372 kW
RORC turbine exergy destruction rate	5.175 kW
Domestic water preheater exergy destruction rate	1.258 kW
Other ingredients exergy destruction rate	0.195 kW
CHP cycle efficiency	12.54 %

Table 10. The results of exergy analysis of the CHP system for the solar and storage mode	
Solar evaporator exergy destruction rate	554.8 kW
RORC evaporator exergy destruction rate	5.372 kW
RORC turbine exergy destruction rate	5.175 kW
Storage heat exchanger exergy destruction rate	3.354 kW
Domestic water preheater exergy destruction rate	1.258 kW
Other ingredients exergy destruction rate	0.241 kW
CHP cycle efficiency	14.86 %

3.1. Effect of varying RORC evaporator pinch point on CHP cycle performance

Fig. 6 shows the variation with RORC evaporator pinch point temperature of the energy efficiency and exergy efficiency for three operation modes. As shown in this figure, increasing RORC evaporator pinch point temperature reduces the heat flow of the RORC evaporator. When the pinch point temperature increases, the heat absorbed by the RORC evaporator decreases so the utilization of this energy decreases, hence the enthalpy of the n-hexane vapour in the RORC evaporator decreases, which reduces the heat flow and eventually leads to a decrease in the energy and exergy efficiencies of the proposed system for three operation modes.

CHP cycle performance

Fig.7 shows the variation of energy efficiency and exergy efficiency with ambient temperature for the solar and solar and storage operation modes. As can be seen, increasing ambient temperature, increases the energy and exergy efficiencies of the proposed system, due to an increase in the ambient temperature, decreases the solar evaporator heat losses and exergy destruction rate for the solar and solar and storage operation modes.

3.2. Effect of varying ambient temperature on CHP cycle performance

Fig.7 shows the variation of energy efficiency and exergy efficiency with ambient temperature for the solar and solar and storage operation modes. As can be seen, increasing ambient temperature, increases the energy and exergy efficiencies of the proposed system, due to an increase in the ambient temperature, decreases the solar evaporator heat losses and exergy destruction rate for the solar and solar and storage operation modes.

3.3 Effect of varying turbine inlet pressure on CHP cycle performance

Table 11. The results of exergy analysis of the CHP system for the storage mode	
Hot storage tank exergy destruction rate	22.77 kW
Storage heat exchanger exergy destruction rate	3.354 kW
Cold storage tank exergy destruction rate	0.03616 kW
RORC evaporator exergy destruction rate	3.262 kW
RORC turbine exergy destruction rate	5.168 kW
Domestic water preheater exergy destruction rate	1.258 kW
Other ingredients exergy destruction rate	0.202 kW
CHP cycle efficiency	47.69 %

Fig.8 shows the variation of energy efficiency and exergy efficiency with CHP cycle turbine inlet pressure for three operation modes. As can be seen, increasing CHP cycle turbine inlet pressure, has no effect on energy efficiency of the overall system. This is due to the range of the CHP cycle turbine inlet pressure. Fig.8 also shows that an increase in CHP cycle turbine inlet pressure enhances the exergy efficiency of the overall system. When the CHP cycle turbine inlet pressure increases, the system total irreversibility decreases so the heating load and net power output of the system increases, hence the small temperature difference between the fluid streams improves the system's performance for three operation modes.

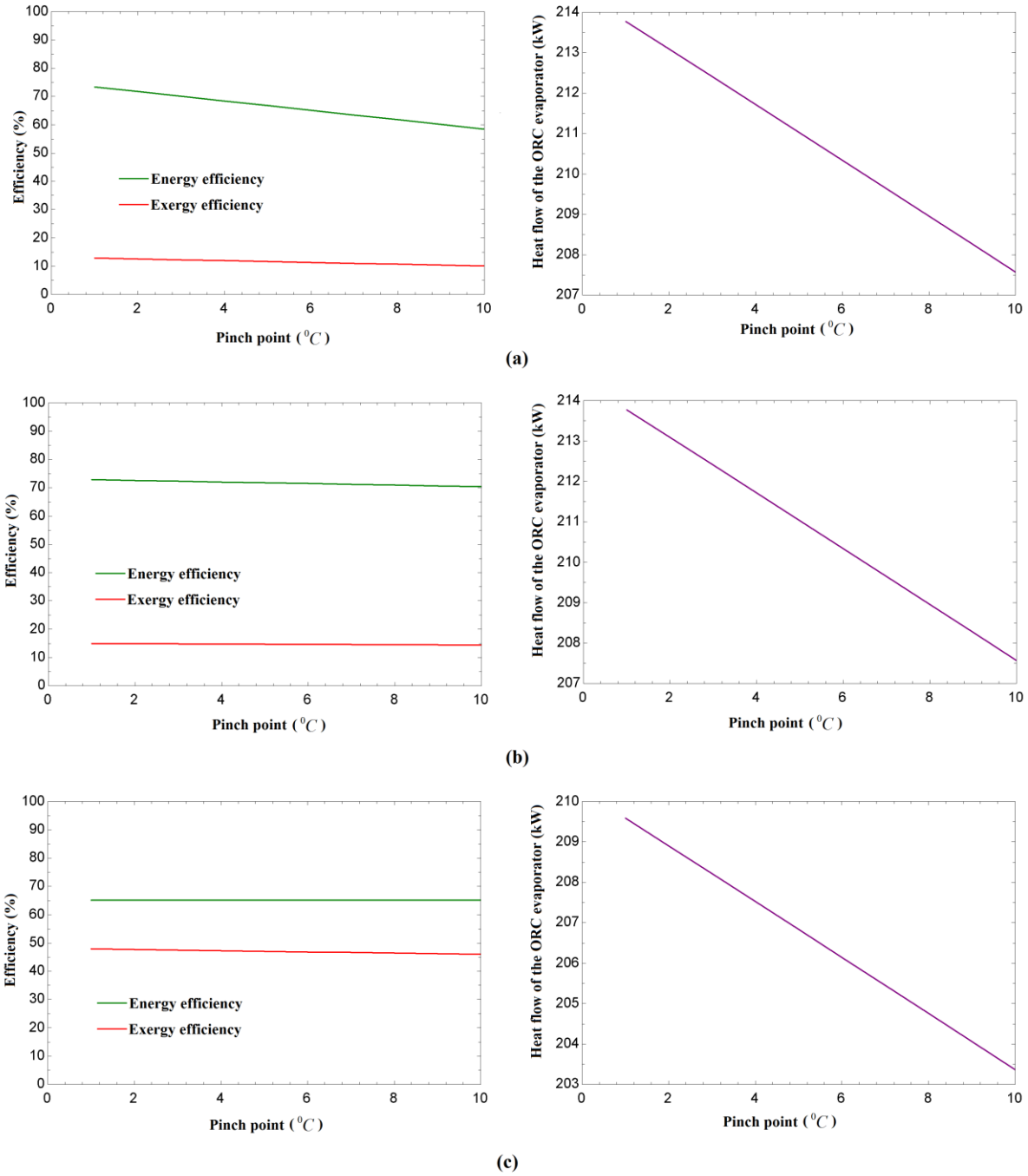

Figure 6. Variation with RORC evaporator pinch point temperature of the energy efficiency and exergy efficiency (a) solar mode, (b) solar and storage mode, (c) storage mode

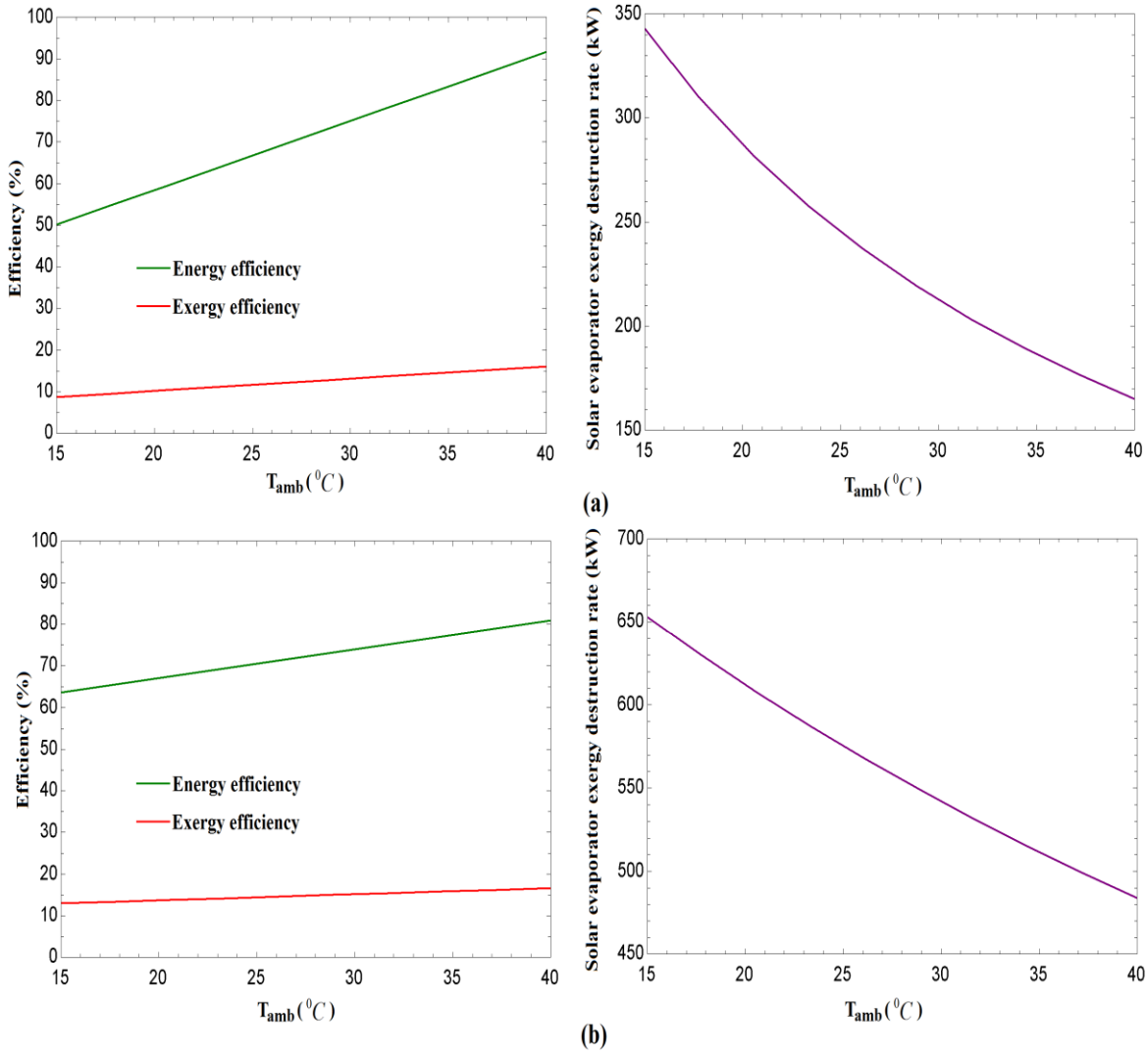

Figure 7. Variation with ambient temperature of the energy efficiency and exergy efficiency (a) solar mode, (b) solar and storage mode

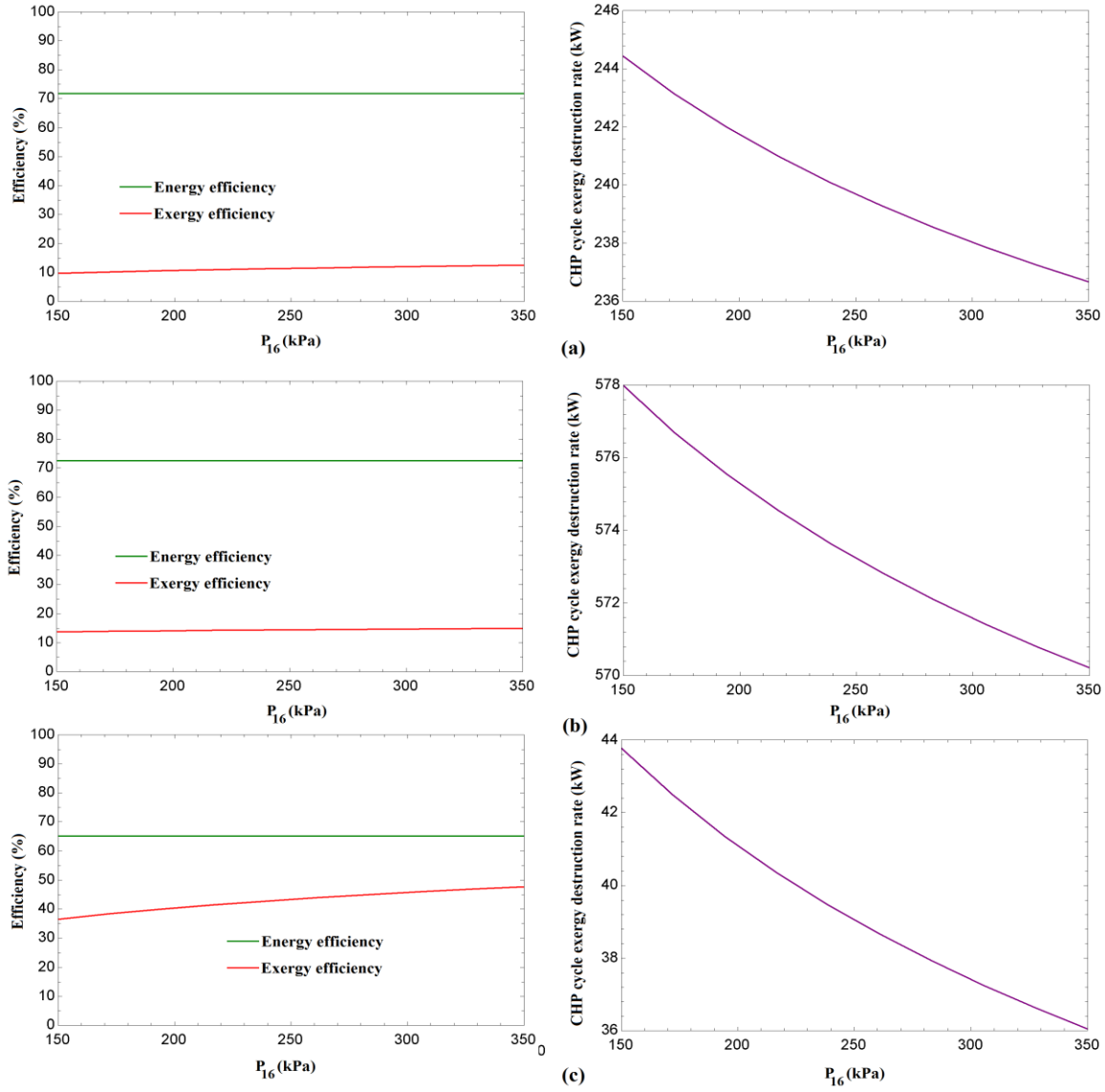

Figure 8. Variation with turbine inlet pressure of the energy efficiency and exergy efficiency (a) solar mode, (b) solar and storage mode, (c) storage mode

4. Conclusions

In this study, the steady state thermodynamic analysis of the solar driven CHP system for three operation modes is conducted under Tabriz summer conditions.

The major aim of this study is the finding, expansion, and modelling of a new solar system with loop heat pipe solar evaporator and introducing a low cost and sustainable and renewable novel solar thermal system for cleaner production of heating, power and cooling. Loop heat pipe has potential to prevail the difficulties in the conventional solar thermal systems and is expected to be low cost, long time life cycle and highly efficiency.

The results of thermodynamic analysis showed that the main source of the exergy destruction is the solar loop heat pipe evaporator for the solar and solar and storage operation modes. In the solar loop heat pipe evaporator, more than 80% of the input exergy was destroyed. Other main sources of exergy destruction are the RORC evaporator, then the RORC turbine and the domestic water preheater. The results also showed that, the storage mode has maximum exergy efficiency and

minimum exergy destruction rate. We can extract some concluding remarks:

- LHPs are the most reliable two phase heat transfer devices, and have very high thermal conductivity.
- Increasing RORC evaporator pinch point temperature leads to a decrease in the energy and exergy efficiencies of the proposed system for three operation modes.
- Increasing ambient temperature, increases the energy and exergy efficiencies of the proposed system, due to an increase in the ambient temperature, decreases the solar evaporator heat losses and exergy destruction rate for the solar and solar and storage operation modes.
- Increasing CHP cycle turbine inlet pressure, has no effect on energy efficiency of the overall system.
- Increasing CHP cycle turbine inlet pressure enhances the exergy efficiency of the overall system.
- The results of this research is useful to understand the performance of the solar loop heat pipe evaporators, create the new layouts related to the design of the solar loop heat pipe systems and promote the solar thermal systems.

Acknowledgements

The author is thankful to the management and staff of NIORDC for their technical and financial support.

Nomenclature

amb	ambient
$A_{SOL,EVA}$	The solar loop heat pipe evaporator area (m^2)
AUX, Pump	Auxiliary pump
CV	control volume
CH,HST	Charging time of the hot storage tank
CHP	combined heating and power
CST	cold storage tank
CH,CST	charging time of the cold storage tank
D_{ll}	Liquid line diameter
D_{vl}	vapour line diameter
D_o	Loop heat pipes outer diameter
δ_w (m)	Thickness of LHPs wicks
δ_{SW} (m)	Thickness of LHPs secondary wicks
δ_{PW} (m)	Thickness of loop heat pipes primary wicks
E	Energy
$\dot{E}$	Exergy rate, kW
E	exit
F, i	fluid entering solar evaporator
F_R	LHP evaporator heat removal factor
G_b	solar radiation, W/m^2
h	specific enthalpy (kJ/kg)
HST	hot storage tank
i	inlet
$\dot{I}$	Exergy destruction rate (kW)
LPRORC, T	low pressure RORC turbine
LHP	loop heat pipe
L_{ll}	Liquid line length
L_{vh}	Vapour header length
L_{vl}	Vapour line length
L_e	Solar evaporator length
$\dot{m}$	Mass flow rate (kg/s)
m_f (Kg)	solar evaporator liquid filling mass
N_{LHP}	number of loop heat pipes
RORC, P	RORC pump
RORC, T	RORC turbine
(Np)	Number of wicks pores
$\dot{Q}$	Heat rate, kW
$\dot{Q}_{FL}(kW)$	Filled liquid Mass limit
$\dot{Q}_{SL}(kW)$	Sonic limit
$\dot{Q}_{EL}(kW)$	Entrainment limit
$\dot{Q}_{BL}(kW)$	Boiling limit
$\dot{Q}_{VL}(kW)$	Viscous limit
REG	Regenerator
RRORC	Regenerative organic rankine cycle
s	specific entropy (kJ/kg-K)
SLHPS	solar loop heat pipe system
SOL, EVA	solar loop heat pipe evaporator
S	radiation absorbed by the solar LHP evaporator
ST,HEX	storage heat exchanger
ST,PUMP	storage pump
SUN	Sun
T_{SUN}	Sun temperature (K)
T	temperature ^0C or K
t	time
u	useful
U_l	Overall heat loss coefficient from LHP to ambient, kW/m^2 K
V	Volume
$\dot{W}$	Work rate, Kw
$\dot{W}_{Net,T}$	Turbine work rate, Kw
η_{ex}	Exergy efficiency

η_{en}	Energy efficiency
ψ	Specific exergy, kJ/kg
η_{LHP}	LHP optical efficiency
τ	Transmission factor
α	Absorption factor

References

[1] Yunus A. Cengel. (2003). HEAT TRANSFER A Practical Approach. McGraw-Hill.

[2] Iran Renewable Energy and Energy Efficiency Organization Annual report, 2010-2017.

[3] Sunil Kumar Sansaniwal, Vashimant Sharma, Jyotirmay Mathur. (2018). Energy and exergy analyses of various typical solar energy applications: A comprehensive review. Renewable and Sustainable Energy Reviews, 82, 1576-1601.

[4] Yanchao Lu, Jiangjiang Wang. (2017). Thermodynamics Performance Analysis of Solar-assisted Combined Cooling, Heating and Power System with Thermal Storage. Energy Procedia, 142, 3226–3233.

[5] Anish Modi, Fabian Bühler,Jesper Graa Andreasen, Fredrik Haglind. (2017). A review of solar energy based heat and power generation systems. Renewable and Sustainable Energy Reviews, 67, 1047–1064.

[6] Ming Liu, N.H. Steven Tay, Stuart Bell, Martin Belusko, Rhys Jacob, Geoffrey Will, Wasim Saman, Frank Bruno. (2016). Review on concentrating solar power plants and new developments in high temperature thermal energy storage technologies. Renewable and Sustainable Energy Reviews, 53, 1411–1432.

[7] Yunus Emre Yuksel, Murat Ozturk, Ibrahim Dincer. (2016). Thermodynamic performance assessment of a novel environmentally benign solar energy based integrated system. Energy Conversion and Management, 119, 109–120.

[8] Haichao Wang, Wusong Yin, Elnaz Abdollahi, Risto Lahdelma, Wenling Jiao. (2015). Modelling and optimization of CHP based district heating system with renewable energy production and energy storage. Applied Energy, 159, 401–421.

[9] Man Wang, Jiangfeng Wang, Pan Zhao, Yiping Dai. (2015). Multi-objective optimization of a combined cooling, heating and power system driven by solar energy. Energy Conversion and Management, 89, 289–297.

[10] Wei He, Xiaoqiang Hong, Xudong Zhao, Xingxing Zhang, Jinchun Shen, Jie Ji. (2014). Theoretical investigation of the thermal performance of a novel solar loop-heat-pipe facade-based heat pump water heating system. Energy and Buildings, 77, 180–191.

[11] Xingxing Zhang, Xudong Zhao, Jihuan Xu, Xiaotong Yu. (2013). Characterization of a solar photovoltaic/loop-heat-pipe heat pump water heating system. Applied Energy, 102, 1229–1245.

[12] Xudong Zhao, Zhangyuan Wang, Qi Tang. (2010). Theoretical investigation of the performance of a novel loop heat pipe solar water heating system for use in Beijing, China. Applied Thermal Engineering, 30, 2526-2536.

[13] Xingxing Zhang, Xudong Zhao, Jihuan Xu, Xiaotong Yu. (2013). Study of the heat transport capacity of a novel gravitational loop heat pipe. International Journal of Low-Carbon Technologies, 8, 210–223.

[14] John A. Duffie, William A. Beckman. (2013). Solar Engineering of Thermal Processes. New York: Wiley.

[15] E. Azad. (2012). Assessment of three types of heat pipe solar collectors. Renewable and Sustainable Energy Reviews, 16, 2833– 2838.